A comparison of Jason-2 plasmasphere electron content measurements to ground-based measurements

Andrew J. Mazzella, Jr.¹, Endawoke Yizengaw²

¹Watertown, Massachusetts, 02472–1049, USA

²Space Science Application Laboratory, The Aerospace Corporation, El Segundo, California, 90245, USA *Correspondence to:* Andrew J. Mazzella, Jr. (ajmazzella@brandeis.edu)

Abstract. Previous studies utilizing the Global Positioning System (GPS) receivers aboard Jason satellites have performed measurements of plasmasphere electron content (PEC) by determining the total electron content (TEC) above these satellites, which are at altitudes of about 1340 km. This study uses similar methods to determine PEC for the Jason–2 receiver for 24 July 2011. These PEC values are compared to previous determinations of PEC from a chain of ground–based GPS receivers in Africa using the SCORPION method, with a nominal ionosphere–plasmasphere boundary at 1000 km. The Jason–2 PECs with elevations greater than 60° were converted to equivalent vertical PEC and compared to SCORPION vertical PEC determinations. In addition, slant (off–vertical) PECs from Jason–2 were compared to a small set of nearly co–aligned ground–based slant PECs. The latter comparison avoids any conversion of Jason–2 slant PEC to equivalent vertical PEC, and can be considered a more representative comparison. The mean difference between the vertical PEC (ground–based minus Jason–2 measurements) values is 0.82±0.28 TEC units (1 TEC unit = 10¹⁶ electrons m⁻²). Similarly, the mean difference between slant PEC values is 0.168±0.924 TEC units. The Jason–2 slant PEC comparison method may provide a reliable determination for the plasmasphere baseline value for the ground–based receivers, especially if the ground stations are confined to only mid–latitude or low–latitude regions, which can be affected by a non–negligible PEC baseline. Keywords: Instruments and techniques, Plasmasphere

15 1. Introduction

The plasmasphere is a toroidal domain of cold plasma confined by the Earth's magnetic field and replenished by the ionosphere (e.g., Lunt et al., 1999a; Dent et al., 2006). Several instruments and methods have been utilized to determine the electron or ion content of the plasmasphere. Among these are the IMAGE (Imager for Magnetopause–to–Aurora Global Exploration) satellite Radio Plasma Imager (Galkin et al., 2004) and Extreme Ultraviolet imager (Sibanda et al., 2012),

- ground-based magnetometers (Dent et al., 2006), satellite-borne Global Positioning System (GPS) receivers for Jason-1 (Yizengaw et al., 2008; Lee et al. 2013) and CHAMP (CHAllenging Minisatellite Payload) (Gerzen et al., 2015), satellite-based tomography (Spencer and Mitchell, 2011), and ground-based GPS receivers using data assimilation (Scherliess et al., 2004) or methods for partitioning total electron content (TEC) into ionosphere and plasmasphere contributions (Mazzella et al., 2002, 2007; Anghel et al., 2009; Carrano et al., 2009).
- More recently, Mazzella et al. (2017) have presented an evaluation of TEC partitioned into the ionosphere and plasmasphere contributions for a chain of GPS receivers in Africa, for 24 July 2011. Peak equivalent vertical ionosphere electron content (VIEC) ranged from about 14 TEC units (1 TEC unit = 10¹⁶ electrons m⁻²) at the southernmost (most poleward) station to about 32 TEC units for near–equatorial stations, while derived peak vertical plasmasphere electron content (VPEC) ranged from about 1 TEC unit to about 6 TEC units for these stations.
- 30 The ground-based TEC study for Africa was conducted using an extension of the Self-Calibration Of Range Error (SCORE) method (Bishop et al., 1994). SCORE employed consistency conditions for equivalent vertical TEC (VTEC) measurements at associated ionosphere penetration points (IPPs) for different lines-of-sight to determine the combined GPS satellite and

ground-based GPS receiver biases. However, as noted by Lunt et al. (1999b) and Fremouw et al. (1998), the occurrence of significant plasmasphere electron content (PEC) affects this calibration process, producing systematic bias errors, with a latitudinal dependence for the sign and magnitude of the errors. Consequently, the SCORE method was generalized by the inclusion of a parametric representation of the plasmasphere, becoming SCORE for Plasmasphere and IONosphere (SCORPION) (Mazzella et al., 2002, 2007). The consistency conditions at associated IPPs were retained by SCORPION, but applied using only the VIEC values, derived from the slant (off-vertical) TEC after removal of the parameterized slant PEC for the corresponding lines-of-sight. The parameters for the plasmasphere representation are determined within the same process as the GPS biases.

Regarding the Africa study, utilization of a chain of receivers with overlapping coverage not only provides extensive latitudinal coverage, but also enables an evaluation of consistency for diurnal VIEC and VPEC profiles between locations and determination of the "plasmasphere baseline". The "plasmasphere baseline" is the local (at each station) spatially and temporally constant component of the observed slant plasmasphere electron content (SPEC). Its value is somewhat affected by limitations for the observational circumstances (the sky regions above the elevation threshold and the typical one–day data coverage). This component can masquerade as a contribution to the receiver bias (Mazzella et al., 2007).

15 The ambiguity between the contributions of the plasmasphere baseline and the receiver bias to the raw measured GPS TEC arises from the formulation for the corrections to the GPS TEC measurements to obtain the VIEC:

STEC = raw GPS slant TEC measurement,

10

20

25

30

SPEC = slant plasmasphere electron content,

Bias = combined receiver and GPS satellite bias, and

SIFac (slant factor) = ratio of slant ionosphere electron content (SIEC) to VIEC.

The slant factor is typically a function solely of the elevation angle () of the GPS satellite at the receiver station, using a representative "thin-shell" altitude (H_s) for the ionosphere (e.g. Lanyi and Roth (1988), in an alternative equivalent mathematical form):

$$SlFac \quad \sec \left(\frac{R \cos \left(\frac{R \cos \left(\frac{e}{R_e H_s} \right)}{R_e H_s} \right)}{R_e H_s} \right)$$
 (2)

where R_e = Earth's radius. In the SCORPION method, the SPEC is represented by a parametric model, with the values of the parameters being determined together with the biases from consistency conditions for the entire set of VIEC values (Mazzella et al., 2002). Because the plasmasphere contribution appears only in combination with the biases, a latitudinal chain or some other external condition must be utilized to appropriately apportion the (local) spatially and temporally constant component between the plasmasphere and the bias. (Note that this is true even if the plasmasphere representation has a unique relationship between the spatially/temporally varying plasmasphere amplitude and the baseline contribution,

because the actual plasmasphere is not governed by such a relationship. This latter ambiguity has been denoted as the "evil twin" problem.)

This subsequent analysis, similar to that performed by Yizengaw et al. (2008) and Lee et al. (2013), has been conducted using Jason–2 GPS receiver data, specifically for Africa on the same day (24 July 2011, 2011–205) as the previous ground–5 based case study (Mazzella et al., 2017) to evaluate PEC values for comparison to those SCORPION results. However, the Jason–2 orbital altitude is approximately 1340 km, and its PEC measurements only correspond to altitudes above this orbital altitude, while the SCORPION measurements incorporate a nominal ionosphere–plasmasphere boundary at 1000 km altitude (Mazzella, 2009). Thus, the SCORPION PEC measurements should be greater than the Jason–2 PEC measurements, but the magnitude of this difference can vary with the time allowed for replenishment of the plasmasphere, the level of solar flux, and even the directions of the lines–of–sight through the plasmasphere (associated with the magnetic field–line crossings and the varying distance to the plasmapause). (See, for example, Fig. 5 by Mazzella (2009).)

2. Data analysis

2.1 Preliminary processing

The Jason-2 GPS receiver data were obtained from the Jet Propulsion Laboratory (JPL) (Komjathy and Haines, private communication, 2013) in Receiver INdependent EXchange (RINEX) format, and were processed using components of the GPS Toolkit (GPSTk) developed by the Applied Research Laboratories (ARL) of the University of Texas at Austin (Tolman et al., 2004). The resulting TEC values (in TEC units) were further adjusted for relative GPS satellite biases, using the August 2011 values from the Center for Orbit Determination in Europe (CODE) of the Astronomical Institute of the University of Bern (Schaer and Feltens, 1998). (As noted by Mazzella et al. (2017), the August 2011 bias value for PRN 1 appeared to be more accurate than the July 2011 value, which was derived soon after the satellite launch.) These GPS TEC tabulations, separated into contiguous time segments for each GPS satellite, were reviewed and edited for any observed anomalies.

A separate component of the GPSTk was utilized to process the same RINEX file for the Jason–2 satellite locations, in three dimensions. The derived latitudes and longitudes were subsequently compared to those in the Geophysical Data Record (Dumont et al., 2011), with good agreement, and the derived radial coordinates were within 4 km of the semi–major axis value (7,714.43 km) reported in the OSTM/Jason–2 Products Handbook (Dumont et al., 2011). The Jason–2 latitude and longitude values were matched to the corresponding GPS TEC samples, and augmented TEC tabulations were generated.

2.2 TEC calibration

25

For each of the contiguous GPS TEC data segments, the dispersive carrier phase (SP) was aligned to the dispersive group delay (SR), using unweighted averaging, to take advantage of the lower noise and multipath associated with the SP values. Because the intrinsic multipath profile for Jason–2 was quite good (Fig. 1), the multipath consistency correction (Andreasen

et al., 2002) used for the ground-based receivers in Africa (Mazzella et al., 2017) was not applied. (This correction process also would have required information about the Jason-2 satellite attitude, to convert the GPS lines-of-sight into a satellite-referenced coordinate system, and further allowance for the effects of the Jason-2 solar panels, as potentially varying multipath contributors.)

The remaining determination of the Jason–2 receiver bias invoked the assumption that the minimum true SPEC is near zero, a method similar to that described by Yizengaw et al. (2008) and Lee et al. (2013), but with the additional consideration of the residual high–altitude, high–latitude electron content, using a model (Pedatella and Larson, 2010). The polar regions were specifically chosen for the receiver bias determination because these were the regions with the intrinsically smallest SPEC values and any model corrections would also be small, so that model errors would have less influence.

Figure 2 displays a north–south cross–section for Jason–2 (latitude 66°) and two GPS satellites (latitude 55°) at their (north) polar extremes, to demonstrate both the lines–of–sight through the polar region and the associated elevation angles at the receiver. The innermost circle is the surface of the Earth, and the radial coordinate is gridded in Earth radius increments. Based on the geometry shown in Fig. 2, two subsets of the Jason–2 receiver data were selected, with one for each polar region. The selection criteria were:

absolute value of Jason–2 latitude \geq 60°; poleward azimuths for lines–of–sight, within \pm 90° of the pole direction;

elevations above 0° for lines-of-sight to the GPS satellites;

absolute value of GPS satellite latitudes ≥ 45°.

30

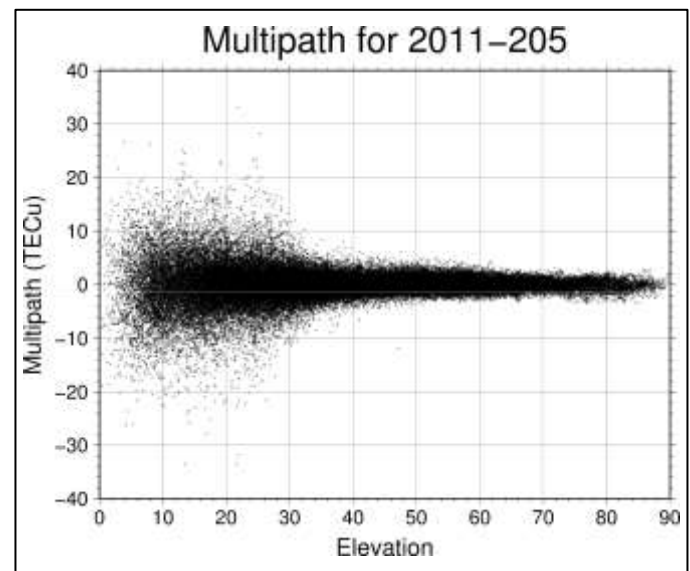


Figure 1. Multipath profile, in TEC units (TECu), for the Jason-2 satellite, derived from its GPS receiver data for 2011–205, using the differences of the SR and aligned SP.

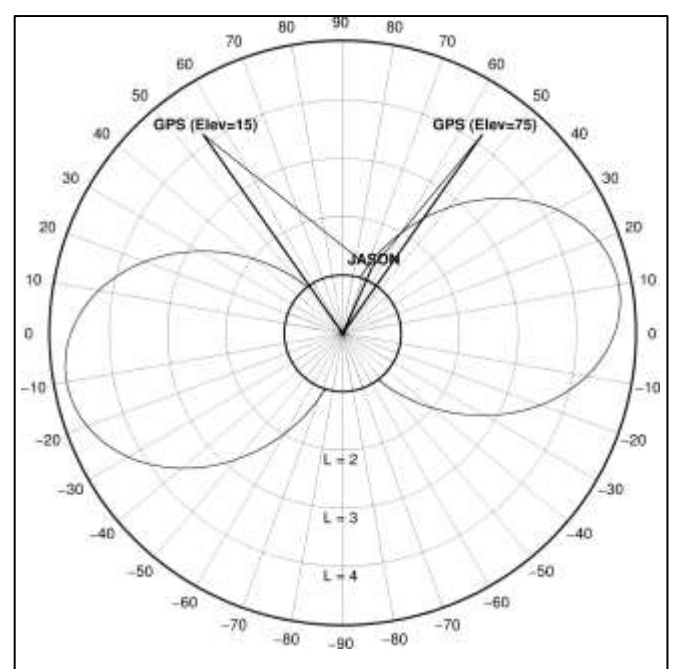


Figure 2. Viewing geometry for minimal expected SPEC occurrences for the Jason-2 GPS receiver, with a representative plasmapause indicated for L=4.8. The low-elevation, cross-polar line-of-sight can mainly avoid the plasmasphere, while the high-elevation line-of-sight can encounter the fringe of the plasmasphere, depending on the relative orientation of the geographic and geomagnetic poles.

The poleward azimuth criterion is intended to eliminate cases like the "Elev=75" case displayed in Fig. 2, which would have the possibility of grazing the plasmasphere, although an alternative criterion could be formulated using magnetic coordinates to avoid the plasmasphere. After consideration of several models, the Parameterized Ionospheric Model (PIM) (Daniell et al., 1995) with the 1988 Gallagher model (Gallagher et al., 1988) was selected for use in this bias determination.

- 5 For the selected polar region data samples, the corresponding model SPEC values were calculated. Additionally, the median altitude for the model cumulative slant PEC, and its associated latitude, longitude, and vertical PEC were calculated. This associated model vertical PEC was calculated for the latitude and longitude of the median altitude location.
 - For each contiguous GPS satellite time segment in the polar region, the minimum SPEC was compared to the minimum model SPEC (from PIM). These results are displayed in Fig. 3 (south polar region, left; north polar region, right). The panels from bottom to top depict the uncalibrated GPS SPEC measurement (SP), PIM SPEC (MdlSPEC), and SP minus MdlSPEC (PECdiff). The minimum PECdiff for the two panels occurs for PRN 17 for the south polar region, with a value of 16.928 TEC units, so this value was provisionally assigned as the receiver bias. The associated minimum SP value is 16.949 TEC units, so the receiver bias cannot be greater than this value without producing negative SPEC values.

10

All of the contiguous GPS satellite segments observed by the Jason-2 receiver were surveyed, for possible SPEC values smaller than that measured for the polar regions. One short (8 minute), low elevation (below 7°) segment for PRN 19 was

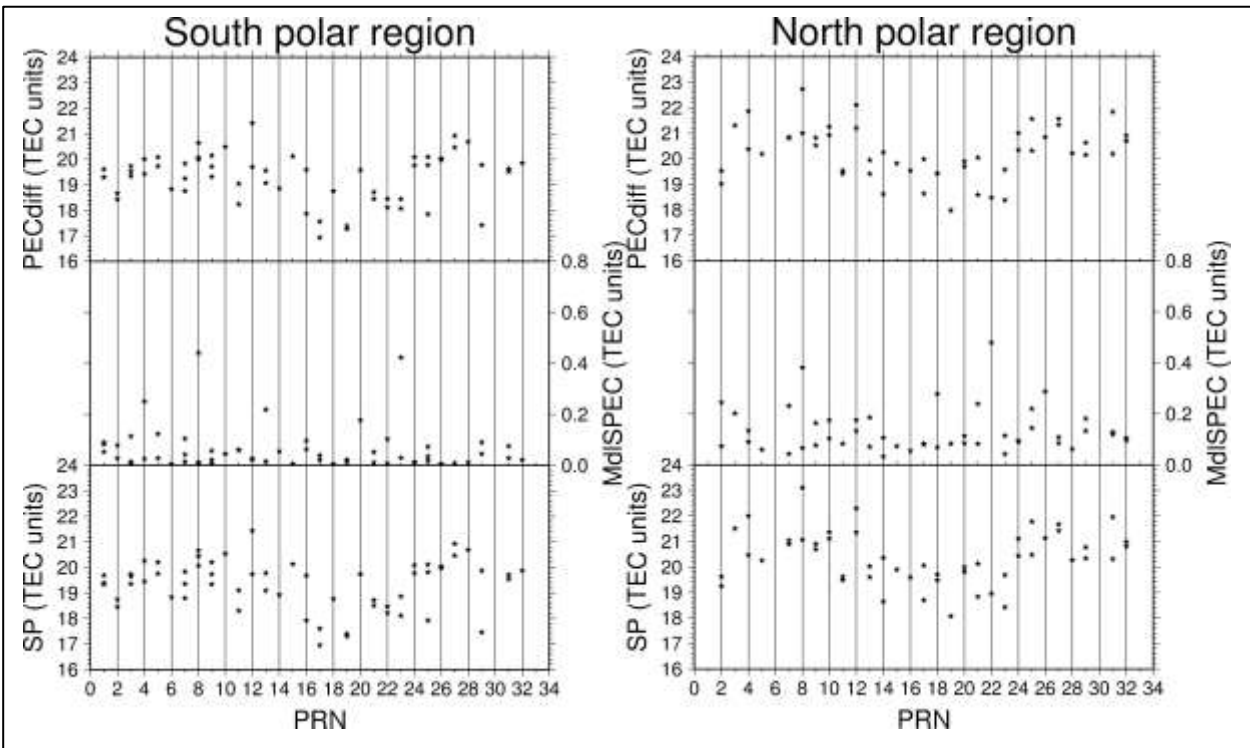


Figure 3. Comparisons for minimum Jason-2 uncalibrated GPS SPEC (SP) values to minimum PIM SPEC (MdlSPEC), for contiguous GPS satellite segments in each polar region, with the corresponding differences PECdiff=SP-MdlSPEC, for each GPS PRN number.

noted, with SPEC values near 14 TEC units, but the estimated error for the alignment of the SP and SR values was about 0.9 TEC units, so this minimum SP was not considered reliable, and this data segment was excluded. The derived receiver bias value was then applied to all of the remaining Jason–2 satellite SPEC data.

An assessment of the receiver bias error was performed through examination of cumulative distribution of derived SPEC values. Figure 4(a) displays the cumulative distribution of SPEC values calculated from PIM. The sharp increase in the distribution for SPEC values near zero indicates a large 15 percentage of SPEC occurrences within a small range of SPEC values ($0 \le SPEC \le 0.2$). However, if there are measurement errors larger than 0.2 TEC units associated with SPEC values, this small SPEC range could not arise. This is illustrated in Fig. 4(b), for which Gaussian "noise" with a standard deviation of 0.75 TEC units is added to the data set. The low SPEC end of the cumulative distribution then has a more gradual increase, which closely resembles the low SPEC end of the actual SPEC cumulative distribution, displayed in Fig. 4(c). Detailed characteristics of the low end of the cumulative distribution vary, depending on the standard deviation of the 30 "noise", so the value of 0.75 TEC units was

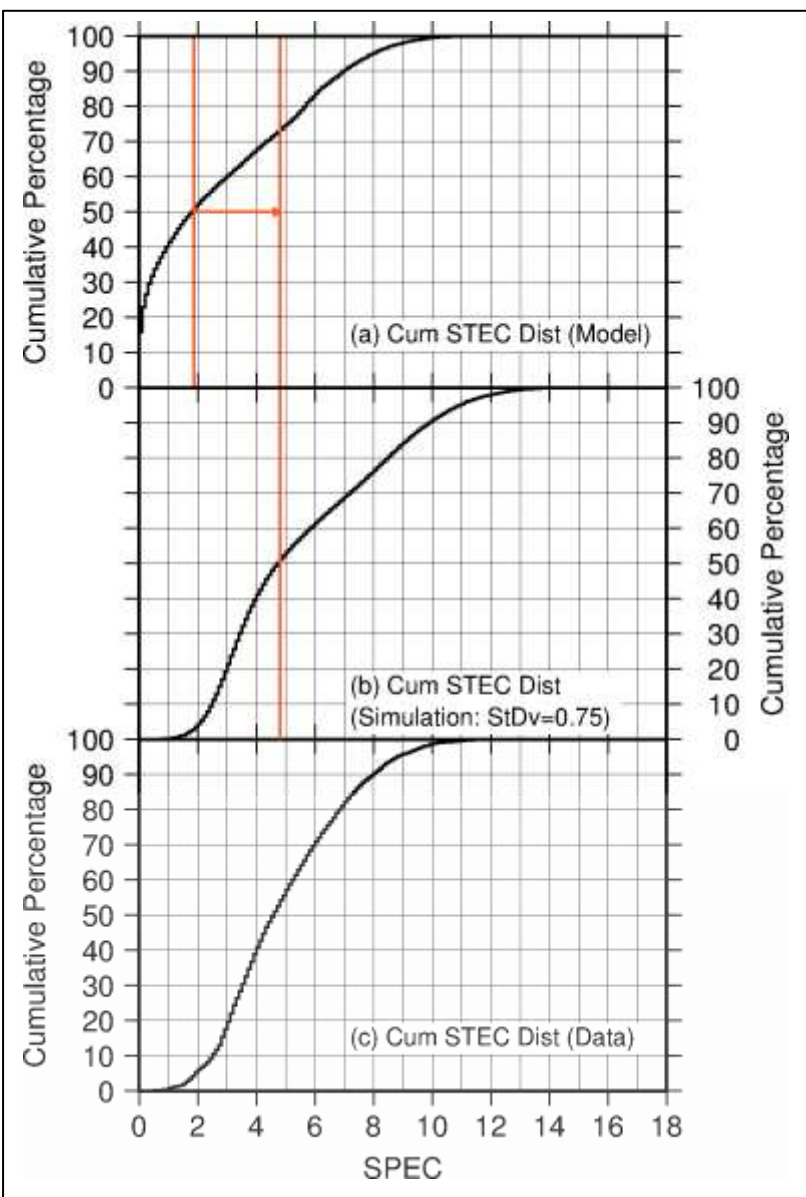


Figure 4. Cumulative distributions for the slant PEC (SPEC) values (in TEC units) from: (a) PIM (for the same lines-of-sight as the data samples); (b) PIM, with added Gaussian "noise", having a standard deviation of 0.75 TEC units; (c) measured, calibrated SPEC data. The vertical red lines indicate the shift of the median of the cumulative distribution for the PIM values, induced by the noise tail at the low end of the distribution.

chosen as the closest match from a set of comparisons. This value was designated as the initial error for the Jason–2 receiver bias. Because the actual low SPEC end of the cumulative distribution is unlikely to be so steep, arising from a sharp high–latitude plasmapause limit and a limited ionosphere extension, the estimate for the SPEC error is a probable upper bound. It

is noteworthy that this error estimate is larger than the typical error range of 0.1–0.3 TEC units arising from the alignment of the SP values to the SR values, which is one of the sources contributing to this error.

A distinct feature occurring between the two simulation panels (Fig. 4(a) and 4(b)) is the shift of the median value for the cumulative distribution, indicated by the two red lines, arising from the noise tail at the low end of the distribution and especially from the lowest value in the noise tail. To evaluate this effect, simulations were performed for 25 separate cases of added noise, all from Gaussian distributions with a standard deviation of 0.75 TEC units. For these cases, the median value of the distribution shifts was 2.962 TEC units, the mean value of the distribution shifts was 2.986 TEC units, and the standard deviation of the distribution shifts was 0.181 TEC units (for a distinctly non–Gaussian distribution of shift values). The median value of the distribution shifts (2.962) was used for the bias adjustment, rather than the mean value (2.986) because of this non–Gaussian distribution of shift values, producing a revised bias value of 19.890 TEC units. The standard deviation of the distribution shifts was combined with the noise standard deviation to give an estimated bias error of 0.772 TEC units. After this bias correction is applied, 16.8 % of Jason–2 slant PEC values are negative, and the revised cumulative distribution median value is 1.66 TEC units.

For eleven of the simulation cases, the cumulative distributions for the simulated data have median values near those of the actual data, after the minimum SPEC bias correction is applied (as in Fig. 4(c)). For the same simulation cases, the noise tails at the low end of the distributions also match the low end of the data distribution. Thus, the calibration could have been accomplished by determining the difference between the median for the original data (without the preliminary adjustment based on the polar region values) and the median for the original model values (as in Fig. 4(a), without the simulated noise). If an alternative error estimate is available for the bias, the determination of the "noise" standard deviation and the associated noise simulations for the model data could be omitted. However, this would also eliminate the verification of matching the low end of the data cumulative distribution and omit a small correction for the variation of the simulated data median values among cases.

15

30

An alternative statistical bias determination is described by Heise et al. (2005), utilizing an average of the differences between measured and model values to evaluate the bias, for a high–latitude subset of the data. For the combined high–latitude data sets selected in this study, their method produces a bias value of 19.846±1.042 TEC units.

A somewhat different method, the "Improved ZERO TEC Method", is described by Zhong et al. (2016), consisting of a daily determination and a correction derived from all days of data. Because only one day of data is analyzed here, only the first part of their evaluation could be applied, involving the minimum SPEC for individual ascending and descending orbital legs. From that evaluation, using the smaller first quartile of the two sets (ascending, descending) of SPEC values, the derived bias shift was 0.618 TEC units, relative to the provisional assignment of 16.928 TEC units. This is significantly less than the value derived above for the median shift, and this result was not used.

Two other calibration methods, the Minimum Standard Deviation method (Valladares et al., 2009) and the SCORE method (Bishop et al., 1994), adapted from ground–based methods, were examined but not used for the data analysis. A description of these evaluations is provided in the Supplement.

Because of the low ion density of the plasmasphere, relative to even the topside ionosphere, and the significant variation of the plasmapause altitude with latitude, the designation of a representative altitude for the usual "thin–shell" formula converting from slant TEC to equivalent vertical TEC was considered problematic (e.g., Mazzella (2009): Fig. 5 and Eq. (1)). Rather than attempting to develop and implement a different formula for the conversion between SPEC and VPEC for all the data, accounting for the satellite altitude and latitude, and the azimuth and elevation of the line–of–sight, PIM was utilized to accomplish this conversion. The PIM SPEC (MdlSPEC) was calculated for all data samples, based on the Jason–2 location and the time, elevation, and azimuth of each of the lines–of–sight. For each sample, the median altitude (MedAlt), for the cumulative slant PEC profile versus altitude, was also evaluated. The associated latitude (MedLat) and longitude (MedLon) for the median altitude occurrence were then determined. The corresponding model vertical PEC (MdlVPEC) was calculated for the (MedLat, MedLon) location, and a representative equivalent vertical PEC for each data sample (EqVPEC) was calculated as

EqVPEC SPcal MdlVPEC/MdlSPEC

(3)

where SPcal is the calibrated GPS SPEC. All of these results were reviewed, graphically.

A composite plot for all the data is displayed in Fig. 5(a), for both the MdlVPEC and EqVPEC versus local time (LT) at the

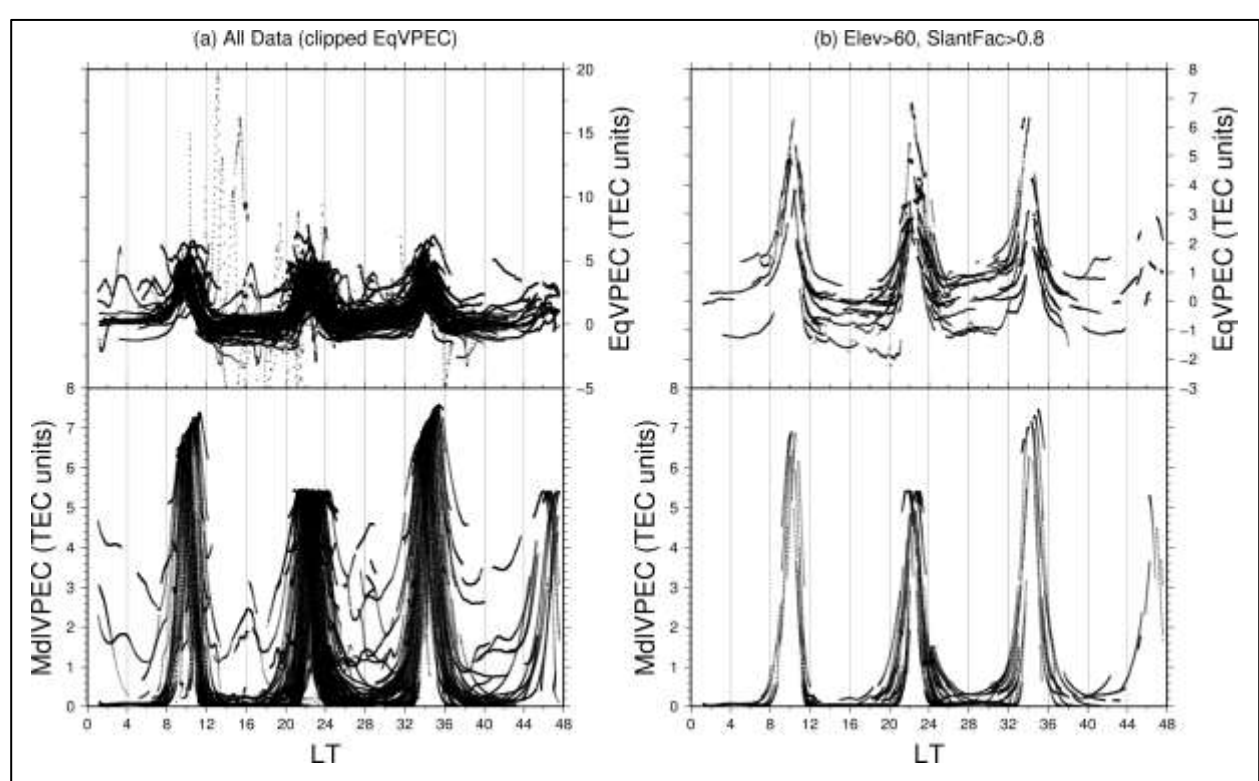


Figure 5. (a) PIM VPEC (MdIVPEC) and equivalent vertical measured PEC (EqVPEC) versus local time (LT) for all data samples (display limited from -5 TEC units for EqVPEC). The minimum EqVPEC value is nearly -36 TEC units, arising from small values for the ratio (SlantFac) of model slant PEC (MdISPEC) to model equivalent vertical PEC (MdIVPEC). (b) MdIVPEC and EqVPEC versus LT for data subset, selected by: $60^{\circ} \le Elevation \le 90^{\circ}$; $0.8 \le SlantFac$.

median altitude location. A [0,24] hour limit is not imposed on the LT evaluations, and continuity in LT is maintained for successive GPS samples, except for the (positive East) longitude discontinuity from 360° to 0° in each orbit. Thus, for the combined Universal Time (UT) and longitude (Lon) progressions (with LT(h) = UT(h) + Lon(deg)/(15 deg h⁻¹)), the LT values extend over [0,48] hours for the 24 hours of Universal Time. The MdlVPEC values display a day/night difference that appears to be absent for the derived EqVPEC results, and the EqVPEC results display many anomalous values. These values are associated with MdlSPEC/MdlVPEC (slant factor) values below 0.8. Consequently, a selected subset of the data was

chosen, and is displayed in Fig. 5(b), with the selection criteria being:

$$-65^{\circ} \le \text{MedLat} \le 65^{\circ}$$

 $60^{\circ} \le \text{Elevation} \le 90^{\circ}$
 $0.8 \le \text{SlantFac}$

10

15

20

(≡ MdlSPEC/MdlVPEC)

Note that, for these selection criteria, the day/night difference is still absent for the measured EqVPEC.

3. Comparisons over Africa

For comparison to the previous groundbased study for Africa, a preliminary regional survey was performed, for the following parameter selections:

$$-60^{\circ} \le \text{MedLat} \le 40^{\circ}$$

 $-10^{\circ} \le \text{MedLon} \le 75^{\circ}$
 $60^{\circ} \le \text{Elevation} \le 90^{\circ}$
 $0.8 \le \text{SlantFac}$

These results are displayed in Fig. 6, for the Jason–2 tracks in the vicinity of Africa (in red) and the associated median altitude occurrences for lines–of–sight to the GPS satellites (in blue). The rings around the displayed subset of sites correspond to a (ground–based) threshold elevation of 35°, intersecting the Jason–2 altitude (1346 km)

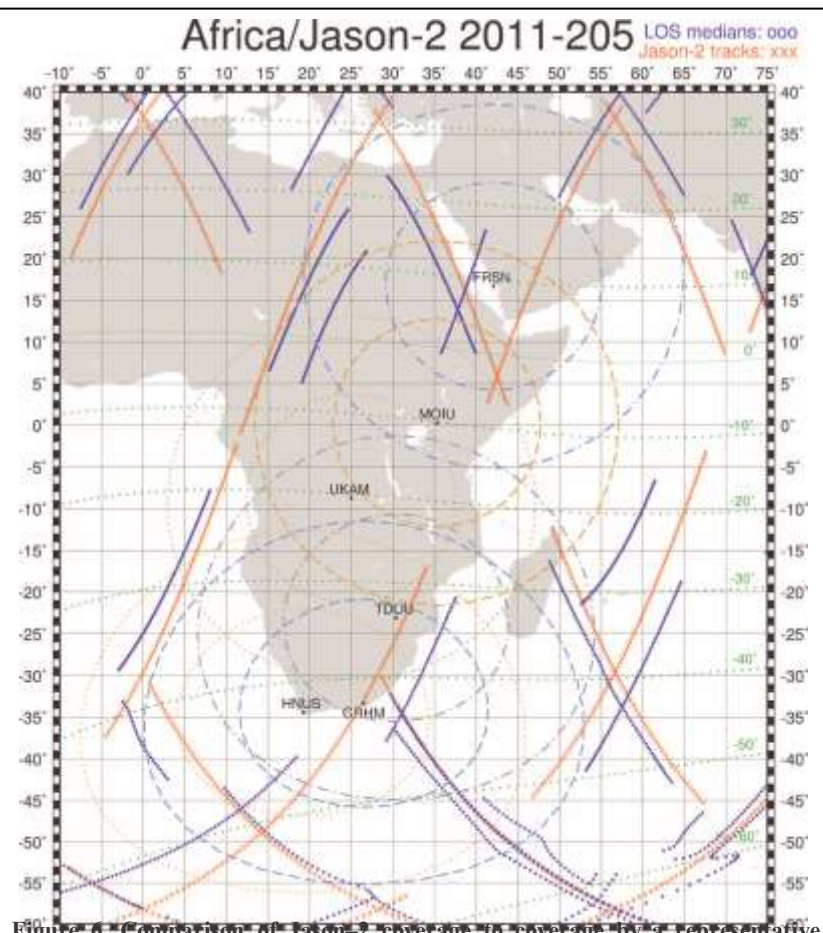


Figure 6. Comparison of Jason 2 coverage to coverage by a representative subset of the ground-based sites for the previous Africa chain study (day 2011–205) (Mazzella et al., 2017). The Jason–2 tracks in the vicinity of Africa are displayed as red tracks (x) and the associated median altitude occurrences for lines–of–sight (LOS) to the GPS satellites are displayed as blue segments (o). The rings around the displayed subset of sites correspond to a threshold elevation of 35°, intersecting the Jason–2 altitude for the inner ring and a representative median altitude for the cumulative line–of–sight slant PEC for the outer ring. The magnetic latitudes displayed within the plot frame are Magnetic Apex Coordinates (VanZandt et al., 1972), appropriate for the ground station locations.

for the inner ring and a representative median altitude (3173 km) for the cumulative line-of-sight slant PEC (as determined from PIM) for the outer ring. Only the Jason-2 line-of-sight median altitude occurrences (blue) within the outer ring for a station are suitable for vertical PEC comparisons for that station. (Note: Not all of the stations in the Africa chain are displayed, to avoid confusion among the rings, but the subset displayed reasonably represents the regional coverage of all of

5 the stations.)

10

15

Because of the high inclination (66.04°) of the Jason–2 orbit, the satellite passages over Africa occur primarily for magnetic local times around 11:00 (for southward passes) and 23:00 (for northward passes) for this day, using the ground station magnetic local time selection conventions previously employed by Mazzella et al. (2017). Data for these two periods, within a half–hour of the nominal magnetic local times, were selected for both the Jason–2 GPS data and the GPS data for each of the ground stations used for the African chain, which are listed in Table 1 (Mazzella et al., 2017), together with their plasmasphere baseline values, in TEC units. The Jason–2 equivalent vertical PEC (EqVPEC) and ground–station plasmasphere vertical electron content (VPEC) derived by the SCORPION method are displayed in Fig. 7 (top panels) as latitudinal profiles, together with the ionosphere vertical electron content (bottom panels) and composite ionosphere and plasmasphere vertical electron content (middle panels) derived by SCORPION. The error bars in Fig. 7 for the ground–based TEC measurements are calculated in the manner described by Mazzella et al. (2017), while the Jason–2 TEC error bars are derived from the analysis for Fig. 4, based on the Gaussian "noise" (0.75 TEC units) required to reproduce the cumulative distribution for the Jason–2 TEC data. The Jason–2 EqVPEC values are less than the corresponding SCORPION VPEC

Table 1. The sites used for the Africa chain study, plus the auxiliary sites Kerguelen Islands and Grahamstown, from south to north, with their supporting networks, and their derived plasmasphere baseline values (in TEC units). (Mazzella et al., 2017)						
Lon (+E)	Lat (+N)	MLat (+N)	ID	Network	Site Name	Baseline
70.256	-49.351	-58.280	KERG	IGS	Kerguelen Islands	0.000
19.223	-34.424	-42.663	HNUS	IGS	Hermanus, South Africa	0.000
26.507	-33.320	-42.259	GRHM	TRIGNET	Grahamstown, South Africa	0.000
20.810	-32.380	-41.324	SUTH	IGS	Sutherland, South Africa	0.000
25.540	-25.805	-36.270	MFKG	IGS	Mafikeng, South Africa	0.066
30.384	-23.079	-33.893	TDOU	IGS	Thohoyandou, South Africa	0.082
26.016	-15.746	-27.232	TEZI	UNAVCO	Itezi-Tezi, Zambia	0.294
25.003	-8.733	-20.522	UKAM	UNAVCO	Kamina, D.R. Congo	0.370
30.090	-1.945	-13.240	NURK	IGS	Kigali, Rwanda	0.922
35.290	0.288	-10.124	MOIU	UNAVCO	Eldoret, Kenya	1.189
37.561	6.062	-3.398	ARMI	UNAVCO	Arba Minch University, Ethiopia	1.905
37.360	11.600	2.819	BDAR	UNAVCO	Bahir Dar, Ethiopia	1.913
42.102	16.699	9.130	FRSN	UNAVCO	Farasan, Saudi Arabia	1.974

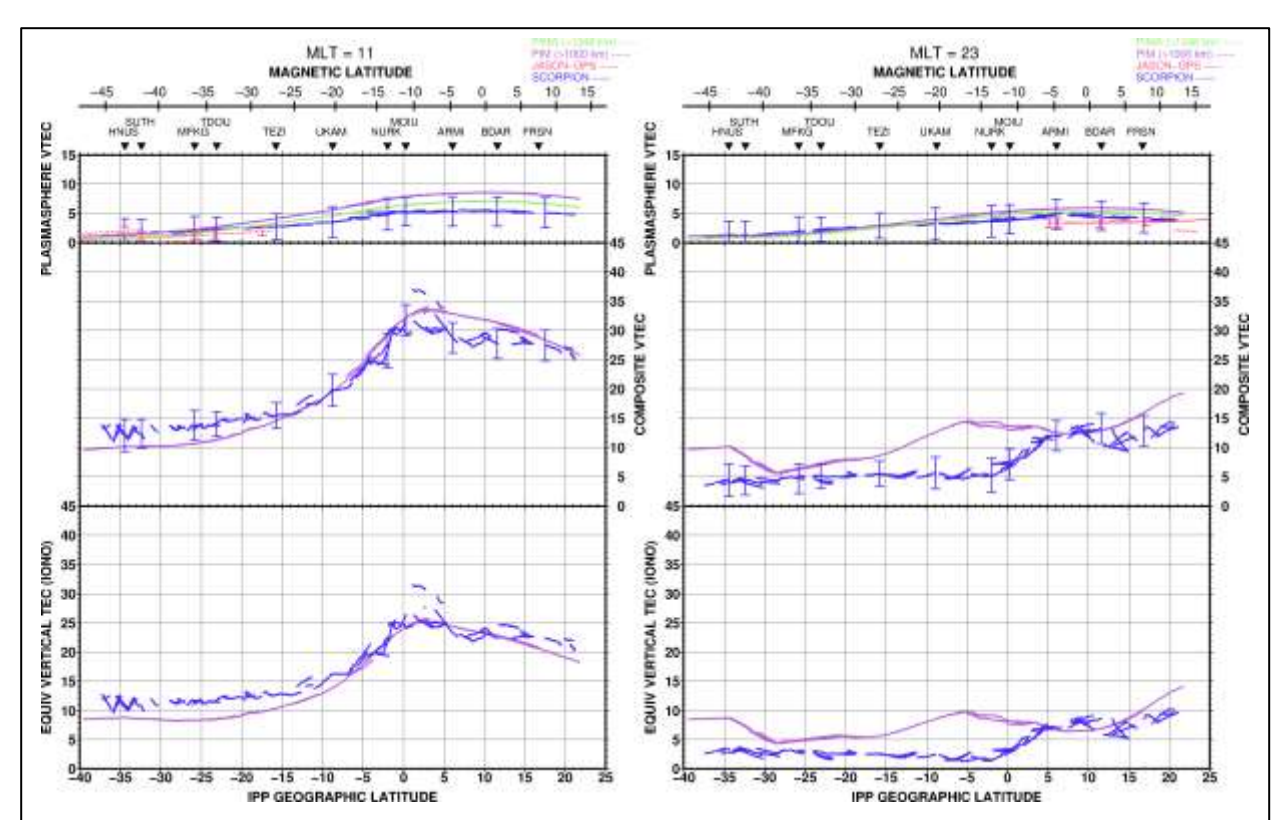


Figure 7. Latitudinal vertical TEC profiles (in TEC units) separately for the ionosphere (bottom panel) and plasmasphere (top panel) (for an ionosphere-plasmasphere boundary at 1000km), with the composite (ionosphere plus plasmasphere) vertical TEC (middle panel), for the SCORPION and PIM results, and for the plasmasphere only for the Jason-2 results (with a base altitude of 1346 km), for Magnetic Local Times 11:00 (left) and 23:00 (right). The corresponding PIM profiles are displayed, for a 1000 km boundary for the ionosphere only (bottom panel) and as the upper PIM profile ("PIM>1000 km)") for the plasmasphere, while the lower PIM plasmasphere profile ("PIMA (>1346 km)") corresponds to an alternative boundary altitude of 1346 km, for comparison to the Jason-2 values.

values, by 0.82±0.28 TEC units, at both high latitudes (daytime samples) and low latitudes (nighttime samples). Because the Jason–2 satellite altitude (1346 km) is greater than that of the nominal ionosphere/plasmasphere boundary (1000 km) used for SCORPION, the Jason–2 EqVPEC is expected to be slightly less than the SCORPION VPEC. From plasmasphere electron content calculated from the PIM/Gallagher model, the vertical PEC between 1000 km and 1346 km ranges from 0.59 to 1.50 TEC units for the daytime period (versus 0.75±0.18 TEC units for SCORPION minus Jason–2) and 0.26 to 0.62 TEC units for the nighttime period (versus 0.91±0.35 TEC units for SCORPION minus Jason–2). The intrinsic VPEC variation determined by SCORPION between the two magnetic local times, and for latitude ranges corresponding to the respective Jason–2 latitudes, is 2.35±0.59 TEC units.

An alternative survey was conducted for Jason-2 data in the vicinity of the ground-based GPS stations, using only the elevation threshold, without the slant factor restrictions associated with Fig. 6. The objective of this survey was to find aligned line-of-sight occurrences, for the same GPS satellite, for Jason-2 and each of the ground stations, so that the

corresponding SPEC measurements could be compared, obviating the requirement for slant-to-vertical conversions for the PEC measurements. The alignment was quantified using the angle between the Jason-2 line-of-sight to the GPS satellite and the ground-based line-of-sight to Jason-2, measured at Jason-2. The angular limit for selection of these occurrences was set as 10°, with a ground-based elevation threshold for Jason-2 designated as 35°. Like the comparison of equivalent vertical PEC measurements, the ground-based SPEC measurements were expected to be slightly larger than the Jason-2 SPEC measurements.

There were two to four ground-based/Jason-2 matches for most of the sites listed in Table 1, with no matches for GRHM and only one for KERG, although as many as three of the matches at a site could be distinct Jason-2 occurrences for nearly-coincident ground-based observations of a single GPS satellite. There were a total of 32 matches for the 10° alignment limit, with the minimum GPS elevation observed by Jason-2 being about 37°, and the minimum ground-based GPS satellite

elevation being about 32°.

An example of alignments for the ground station ARMI is displayed in Fig. 8, indicating the lines-of-sight from the station to Jason-2 (red) and the common GPS satellite (PRN 14) (purple), plus the lines-of-sight from Jason-2 to that GPS satellite (blue). Nominal plasmasphere penetration points for these Jason-2 lines-of-sight are indicated (black dots), based on the median cumulative slant **TEC** calculated from PIM, showing the distance of these penetration points from the location of Jason-2, and the assigned location for the EqVPEC (although the EqVPEC is not used in this comparison). The two cases displayed are the only two alignments for ARMI for day 2011-205, at the 30second sampling of the ground station GPS data. (The two distinct GPS satellite locations are nearly coincident,

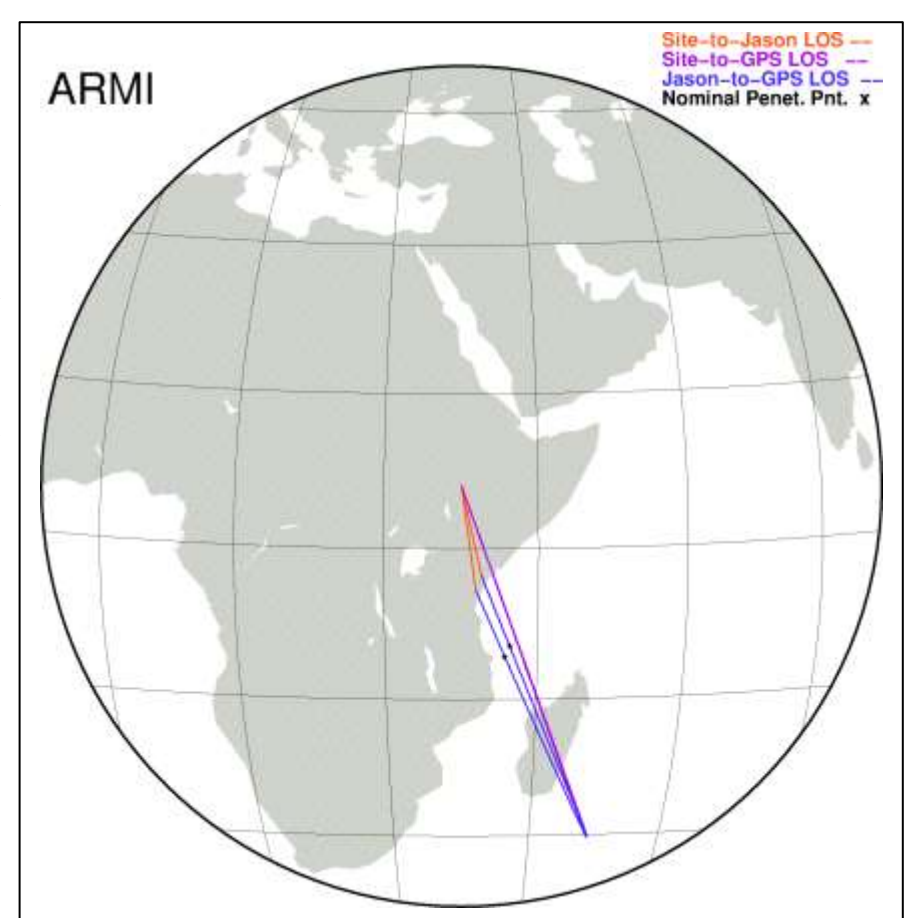


Figure 8. Aligned lines-of-sight from the ground station ARMI to Jason-2 (red) and to the common GPS satellite (PRN 14) observed (purple), plus the lines-of-sight (blue) from Jason-2 to that GPS satellite, with nominal plasmasphere penetration points for the Jason-2 lines-of-sight (black dots), based on the median cumulative slant TEC calculated from PIM. The ground-based elevation of the GPS satellite for the occurrences displayed is about 41°.

and redundant pairings associated with the 10-second Jason–2 data sampling are not utilized.)

For all of the sites, the SPEC comparisons arising from the alignment cases are displayed in Fig. 9 (circles), showing slightly higher SPEC values for the SCORPION ground-based measurements, by about 0.24 TEC units. For comparison, an offset linear fit (Y=A+X) to the data samples, with an intercept of 0.168±0.924 TEC units, is displayed in blue, and a first-order fit (Y=A+B*X), with a slope of 0.921 and 10 an intercept of 0.311±0.920 TEC units, is displayed in red. A tabulation of all the SPEC comparisons and associated parameters is provided in the Supplement, as the data for Fig. 9.

4. Discussion and conclusions 15

30

This study supplements a previous analysis of groundbased GPS TEC measurements over Africa (Mazzella et al., 2017), specifically for comparison of the

Slant PEC Comparison 6 SPEC Fit: Y = A + X SPEC Fit: Y = A + B*X SPEC Data Ground-SPEC (TEC units) 00 2 5 0 Figure 9. SPEJason-SPEC (TEC units) receivers (Ground-SPEC) versus the Jason-2 GPS receiver (Jason-SPEC) (circles), with two alternative linear fits: (Y=A+X) (blue), and

(Y=A+B*X) (red), both indicating intercepts of about 0.24 TEC units.

plasmasphere component of those measurements, by analyzing GPS measurements from a Jason 2 satellite borne receiver

thus intrinsically isolating the plasmasphere contribution. The comparisons were conducted both for the derived EqVPEC 20 determination, which is a secondary quantity produced using several underlying assumptions and conversions, and the SPEC determination, which is a more directly derived quantity, especially for the Jason-2 measurements. The Jason-2 measurements are affected primarily by the receiver bias determination, but also by the relative biases for the individual GPS satellites. This comparison of satellite-based SPEC to ground-based SPEC measurements may be the first such comparison reported or conducted. 25

In addition to the derived Jason-2 receiver bias, the EqVPEC determinations from Jason-2 rely on the relative GPS satellite biases and the conversion of the SPEC measurements to representative EqVPEC values. As noted above, the assessments for the satellite bias for PRN 1 changed significantly (by about 7.6 TEC units) between the July 2011 and August 2011 tabulations by CODE, with the August 2011 value being more consistent with the values derived for the African stations by the SCORPION method for 24 July 2011 (Mazzella et al. (2017): Fig. 8). In this case, the July 2011 PRN 1 bias was underestimated, but an overestimate of the same magnitude would have resulted in the PRN 1 SP values in Fig. 3 becoming the lowest measured SP values, and thus affecting the initial evaluation for the Jason-2 receiver bias (prior to the adjustment

for the median shift). However, all of the PRN 1 high latitude SP values in Fig. 3 would be distinct outliers for such an occurrence, and thus subject to further examination and likely elimination.

The PIM/Gallagher (Daniell et al., 1995; Gallagher et al., 1988) ionosphere–plasmasphere model was used to provide both correction values for the Jason–2 receiver bias determination and slant factors for the conversion from SPEC to EqVPEC for the satellite–based measurements. While some erratic slant factor values (attributed to small MdlSPEC and MdlVPEC values) arose from this process, the oversimplification of a single reference slant factor altitude was circumvented.

For differences taken as ground-based minus Jason-2 measurements, the mean difference for vertical PEC comparisons is 0.82±0.28 TEC units, while the mean difference for SPEC comparisons is 0.168±0.924 TEC units. The large error designated for the SPEC comparisons reflects the small sample count for the comparison pairs and some significant outliers.

The Jason–2 SPEC comparison method may provide a reliable value for the plasmasphere baseline determination for the ground–based receivers, especially if the ground stations are confined to only mid–latitude or low–latitude regions. For these regions, the plasmasphere can provide an apparent spatially constant (over the sky regions above the observational elevation threshold) and temporally constant (over the generally one–day observation period) contribution that can be mistaken as a bias component. The Jason–2 satellite, by sampling high latitude regions with essentially zero plasmasphere electron content, can provide an alternative reference for the baseline ambiguity of the ground–based plasmasphere measurements. This expectation is supported by the close agreement, in Fig. 9, of the offset linear fit to the more general first–order linear fit. However, the applicability of this reference usage is slightly degraded by the difference in the altitudes used by Jason–2 and

However, the applicability of this reference usage is slightly degraded by the difference in the altitudes used by Jason–2 and the ground–based measurements for the plasmasphere lower boundary and the relatively large error bars compared to the tabulated plasmasphere baseline values (Table 1).

With regard to the PIM/Gallagher model, a generally good agreement is obtained with both the Jason–2 and SCORPION vertical PEC results for the nighttime case (Fig. 7, MLT=23), although the Jason–2 measurements are confined to the magnetic equatorial region for this case. The PIM/Gallagher results are also consistent with the Jason–2 and SCORPION vertical PEC results for the high latitude region for the daytime case (Fig. 7, MLT=11), but diverge from the SCORPION results at low latitudes. A notable difference between the vertical PEC results for PIM/Gallagher and either Jason–2 or

SCORPION is the diminished equatorial day/night variation obtained by Jason–2 (Fig. 5) and SCORPION (Fig. 7). (This is further evident for SCORPION from Fig. 4 and 5 by Mazzella et al. (2017).) A similar small day/night variation (about 1 TEC unit) was noted by Lee et al. (2013) for a multi-year study (2002–2009).

Code availability

30

5

The Generic Mapping Tools version 4.5.12 was used in this study; the closest available version is 4.5.18 (accessed 24 June 2021), accessible at Download: https://www.generic-mapping-tools.org/download/.

The GPS Toolkit versions 2.4 and 2.5 were used in this study; the closest available version is 2.12.1 (accessed 24 June 2021), accessible at Releases: https://gitlab.com/sgl-ut/GPSTk/-/releases.

The PIM software, version 1.7, with the Gallagher model, was acquired from https://www.cpi.com/products/pim.html, which is not currently active.

Data availability

Data associated with Fig. 1, Fig. 3–7, and Fig. 9 are provided as text tabulations in the Supplement. (The tabulation for Fig. 5 comprises the entire data set. Figure 8 contains a subset of the data associated with Fig. 9.)

Data corresponding to the Jason-2 RINEX data used for this study are available (accessed 12 August 2022) from Comprehensive Large Array-data Stewardship System (CLASS): http://www.class.noaa.gov/.

The relative GPS satellite biases were obtained from ftp://ftp.unibe.ch/aiub/CODE, which is no longer accessible. An alternative source is http://ftp.aiub.unibe.ch/CODE/ (accessed 06 January 2023).

10 Author contribution

EY proposed this investigation as a corroboration of the ground-based GPS plasmasphere measurements. AJM developed the procedures for data processing and calibration, and the methods and software for comparing the satellite and ground-based measurements. AJM also conducted the processing and comparisons, including preparation of the tabulations and graphical displays. AJM prepared the initial draft of this manuscript, and both EY and AJM reviewed and revised the manuscript for submission.

Competing interests

15

A.J. Mazzella developed the SCORPION method and its predecessor, SCORE. E. Yizengaw declares that he has no conflict of interest.

Acknowledgments

Development of SCORPION was conducted in collaboration with G. Susan Rao and supported by the Air Force Research Laboratory Space Vehicles Directorate under SBIR contracts FA8718–04–C–0009 and FA8718–05–C–0026 to NorthWest Research Associates. Part of E. Yizengaw's work was supported by AFOSR (FA9550–20–1–0119) and NSF (AGS1848730) grants.

The figures were prepared using the Generic Mapping Tools (GMT) graphics (Wessel and Smith, 1998).

The Jason–2 GPS receiver data were provided by A. Komjathy and B. Haines of the Jet Propulsion Laboratory (JPL).

The Jason 2 Geophysical Data Record information was obtained from ftp://avisoftp.cnes.fr/AVISO/pub/jason
2/ssha gdr d/cycle 112/JA2 GPR 2PdP112 183 20110724 190731 20110724 200344.nc.

The authors are grateful to two anonymous referees and the Topical Editor, Dalia Buresova, for their evaluations and comments.

References

- Andreasen, A. M., Holland, E. A., Fremouw, E. J., Mazzella, A. J., Rao, G. S., and Secan, J. A.: Investigations of the nature and behavior of plasma-density disturbances that may impact GPS and other transionospheric systems, AFRL-VS-TR-2003-1540, Air Force Res. Lab., Hanscom Air Force Base, Mass., 2002.
 - Anghel, A., Carrano, C., Komjathy, A., Astilean, A., and Letia, T.: Kalman filter-based algorithms for monitoring the ionosphere and plasmasphere with GPS in near-real time, J. Atmos. Sol.-Terr. Phy., 71, 158–174, doi:10.1016/j.jastp.2008.10.006, 2009.
- Bishop, G., D. Walsh, P. Daly, A. Mazzella, and E. Holland, Analysis of the temporal stability of GPS and GLONASS group delay correction terms seen in various sets of ionospheric delay data, Rep. ION GPS-94, Inst. of Navig., Washington, D.C., 1994.
 - Carrano, C. S., Anghel, A., Quinn, R. A., and Groves, K. M.: Kalman filter estimation of plasmaspheric total electron content using GPS, Radio Sci., 44, RS0A10, doi:10.1029/2008RS004070, 2009.
- Daniell, R. E., Brown, L. D., Anderson, D. N., Fox, M. W., Doherty, P. H., Decker, D. T., Sojka, J. J., and Schunk, R. W.: PIM: A global ionospheric parameterization based on first principles models, Radio Sci., 30, 1499–1510, 1995.
 Dent, Z. C., Mann, I. R., Goldstein, J., Menk, F. W., and Ozeke, L. G.: Plasmaspheric depletion, refilling, and plasmapause
 - dynamics: A coordinated ground-based and IMAGE satellite study, J. Geophys. Res., 111, A03205 doi:10.1029/2005JA011046, 2006.
- 20 Dumont, J.P., Rosmorduc, V., Picot, N., Bronner, E., et al.: OSTM/Jason-2 Products Handbook, OSTM-29-1237, JPL, 2011.
 - Fremouw, E.J., Holland, E.A., Mazzella, A.J., Jr.: Investigations of the Nature and Behavior of Plasma-density Disturbances That May Impact GPS and Other Transionospheric Systems, AFRL-VS-TR-1999-1515, Air Force Res. Lab., Hanscom Air Force Base, Mass., 1998.
- 25 Galkin, I. A., Reinisch, B. W., Huang, X., Benson, R. F., and Fung, S. F.: Automated diagnostics for resonance signature recognition on IMAGE/RPI plasmagrams, Radio Sci., 39, RS1015, doi:10.1029/2003RS002921, 2004.
 - Gallagher, D. L., Craven, P. D., and Comfort, R. H.: An empirical model of the Earth's plasmasphere, Adv. Space Res., 8(8), 15–24, 1988.
- Gerzen, T., Feltens, J., Jakowski, N., Galkin, I. Denton, R., Reinisch, B. and Zandbergen, R.: Validation of plasmasphere electron density reconstructions derived from data on board CHAMP by IMAGE/RPI data, Adv. Sp. Res., Pages 170–183, Volume 55, Issue 1, doi:10.1016/j.asr.2014.08.005, 2015.

- Heise, S., Stolle, C., Schluter, S., and Jakowski, N., Differential code bias of GPS receivers in low earth orbit: An assessment for CHAMP and SAC-C, in: Earth Observation with CHAMP, edited by C. Reigber, H. Luhr, P. Schwintzer, and J. Wicker, Springer, Berlin, 465–470, doi:10.1007/b138105, 2005.
- Komjathy, A. and Haines, B.: private communication, 2013.
- 5 Lanyi, G., and Roth, T.: A comparison of mapped and measured total ionospheric electron content using global positioning system and beacon satellite observations, Radio Sci., 23(4), 483–492, 1988.
 - Lee, H.–B., Jee, G., Kim, Y. H., and Shim, J. S.: Characteristics of global plasmaspheric TEC in comparison with the ionosphere simultaneously observed by Jason–1 satellite, J. Geophys. Res, 118, 1–12, doi:10.1002/jgra.50130, 2013.
- Lunt, N., Kersley, L., and Bailey, G. J.: The influence of the protonosphere on GPS observations: Model simulations, Radio
- Sci., 34, 725–732, doi:10.1029/1999RS900002, 1999a.

 Lunt, N., Kersley, L., Bishop, G. J., Mazzella, A. J., and Bailey, G. J.: The effect of the protonosphere on the estimation of
 - GPS total electron content: Validation using model simulations, Radio Sci., 34, 1261–1271, doi:.1029/1999RS900043, 1999b.
 - Mazzella, A. J., Jr.: Plasmasphere effects for GPS TEC measurements in North America, Radio Sci., 44, RS5014, doi:10.1029/2009RS004186, 2009.
 - Mazzella, A. J., Holland, E. A., Andreasen, A. M., Andreasen, C. C., Rao, G. S., and Bishop, G. J.: Autonomous estimation of plasmasphere content using GPS measurements, Radio Sci., 37, 1092–1095, doi:10.1029/2001RS002520, 2002.
 - Mazzella, A. J., Rao, G. S., Bailey, G. J., Bishop, G. J., and Tsai, L. C.: GPS determinations of plasmasphere TEC, paper presented at International Beacon Satellite Symposium, Boston Coll., Boston, Mass, 1–7, 2007.
- 20 Mazzella, A. J., Jr., Habarulema, J. B., and Yizengaw, E.: Determinations of ionosphere and plasmasphere electron content for an African chain of GPS stations, Ann. Geophys., 35, 599–612, doi:10.5194/angeo-35-599-2017, 2017.
 - Pedatella, N. M., and Larson, K. M., Routine determination of the plasmapause based on COSMIC GPS total electron content observations of the midlatitude trough, J. Geophys. Res., 115, A09301, doi:10.1029/2010JA015265, 2010.
 - Schaer, S. and Feltens, J.: IONEX: The IONosphere Map EXchange Format Version 1, in: Proceedings of the IGS AC
- 25 Workshop, Darmstadt, Germany, 9–11 February 1998, 1–15, 1998.
 - Scherliess, L., Schunk, R. W., Sojka, J. J., and Thompson, D. C.: Development of a physics-based reduced state Kalman filter for the ionosphere, Radio Sci., 39, RS1S04, doi:10.1029/2002RS002797, 2004.
 - Sibanda, P., Moldwin, M. B., Galvan, D. A., Sandel, B. R., and Forrester, T.: Quantifying the azimuthal plasmaspheric density structure and dynamics inferred from IMAGE EUV, J. Geophys. Res., 117, A11204, doi:10.1029/2012JA017522,
- 30 2012.

15

Spencer, P. S. J., and Mitchell, C. N.: Imaging of 3–D plasmaspheric electron density using GPS to LEO satellite differential phase observations, Radio Sci., 46, RS0D04, doi:10.1029/2010RS004565, 2011.

- Tolman, B., Harris, R. B., Gaussiran, T., Munton, D., Little, J., Mach, R., Nelsen, S., Renfro, B., and Schlossberg, D.: The GPS toolkit—Open source GPS software, paper presented at: 17th International Technical Meeting, Satell. Div., Inst. of Navig., Long Beach, Calif., Sept. 2004.
- Valladares, C. E., Villalobos, J., Hei, M. A., Sheehan, R., Basu, Su., MacKenzie, E., Doherty, P. H., and Rios, V. H.:
- 5 Simultaneous observation of travelling ionospheric disturbances in the Northern and Southern Hemispheres, Ann. Geophys., 27, 1501–1508, doi:10.5194/angeo-27-1501-2009, 2009.
 - VanZandt, T. E., Clarke, W. L., and Warnok, J. M.: Magnetic apex coordinates: A magnetic coordinate system for the ionospheric F2 layer, J. Geophys. Res., 77, 2406–2411, 1972.
- Wessel, P., and Smith, W. H. F.: New, improved version of Generic Mapping Tools released, Eos Trans. AGU, 79(47), 579, doi:10.1029/98EO00426, 1998.
 - Yizengaw, E., Moldwin, M. B., Galvan, D., Iijima, B. A., Komjathy, A., and Mannucci, A. J.: Global plasmaspheric TEC and its relative contribution to GPS TEC, J. Atm. Sol.—Terr. Phys., 70, 1541—1548, doi:10.1016/j.jastp.2008.04.022, 2008.
 - Zhong, J., Lei, J., Yue, X., and Dou, X.: Determination of Differential Code Bias of GNSS Receiver Onboard Low Earth Orbit Satellite, IEEE Transactions on Geoscience and Remote Sensing, 54(8), 4896–4905,
- 15 doi:10.1109/TGRS.2016.2552542, 2016.